Inorganic Chemistry

Article

pubs.acs.org/IC

Low-Spin versus High-Spin Ground State in Pseudo-Octahedral Iron Complexes

David N. Bowman and Elena Jakubikova*

Department of Chemistry, North Carolina State University, Raleigh, North Carolina 27695, United States

Supporting Information

ABSTRACT: Pseudo-octahedral complexes of iron find applications as switches in molecular electronic devices, materials for data storage, and, more recently, as candidates for dye-sensitizers in dye-sensitized solar cells. Iron, as a first row transition metal, provides a weak ligand-field splitting in an octahedral environment. This results in the presence of low-lying ^{5}T excited states that, depending on the identity of iron ligands, can become the ground state of the complex. The small energy difference between the low-spin, ^{1}A, and high-spin, ^{5}T, states presents a challenge for accurate prediction of their ground state using density functional theory. In this work, we investigate the applicability of the B3LYP functional to the ground state determination of first row transition metal complexes, focusing mainly on Fe(II) polypyridine complexes with ligands of varying ligand field strength. It has been shown previously that B3LYP artificially favors the ^{5}T state as the ground state of Fe(II) complexes, and the error in the energy differences between the ^{1}A and ^{5}T states is systematic for a set of structurally related complexes. We demonstrate that structurally related complexes can be defined as pseudo-octahedral complexes that undergo similar distortion in the metal−ligand coordination environment between the high-spin and low-spin states. The systematic behavior of complexes with similar distortion can be exploited, and the ground state of an arbitrary Fe(II) complex can be determined by comparing the calculated energy differences between the singlet and quintet electronic states of a complex to the energy differences of structurally related complexes with a known, experimentally determined ground state.

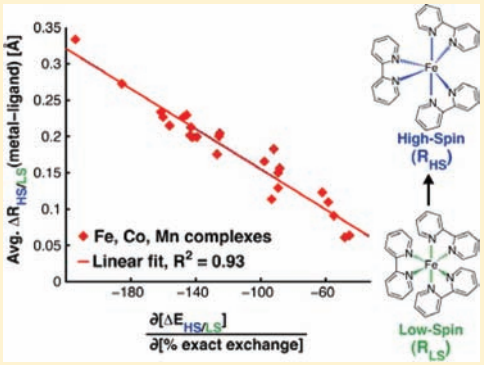

1. INTRODUCTION

Iron pseudo-octahedral complexes have been long considered ideal building blocks for molecular electronic switches, data storage materials, or display devices.[1] Iron, as a first row transition metal, provides a weak ligand field in a pseudo-octahedral environment, which leads to the presence of two energetically close electronic states, ^{1}A and ^{5}T. Depending on the character of ligands coordinated to the central iron metal, the complexes can display either a low-spin (^{1}A), or a high-spin (^{5}T) ground state. The presence of a low-lying excited state of a different spin than the ground state is also responsible for the spin crossover phenomenon in these compounds, in which the complex changes its spin state under the application of an external perturbation such as a change in temperature, pressure, or exposure to electromagnetic radiation.[2]

Fe(II) polypyridine complexes have also been investigated as potential photosensitizers in dye-sensitized solar cells due to their structural resemblance to the Ru(II) polypyridine dyes and the low cost and low toxicity of iron.[3−8] Unfortunately, the spin crossover properties of these compounds complicate their use as photosensitizers, since upon the excitation by visible light into the singlet metal-to-ligand charge transfer states (^{1}MLCT) they quickly undergo intersystem crossing into the manifold of nonphotoactive ^{5}T states.[7−10] Moreover, only complexes with a ^{1}A ground state absorb visible light with appreciable intensity and attain the photoactive ^{1}MLCT states upon excitation.[9,10]

Computational studies of Fe(II) complexes aiming to either obtain a deeper understanding of their electronic structure or to suggest new compounds with desirable properties face a number of challenges. One of these challenges is the correct determination of the ground state, which is nontrivial.[11,12] There have been a number of computational studies dedicated to spin crossover compounds using density functional theory (DFT)[12−20] as well as higher levels of theory, such as CASPT2 (complete active space with second-order perturbation theory).[21,22] Due to the size of these systems (50 or more atoms), they are most amenable to calculations performed by DFT methods. While DFT is very successful at predicting geometries of both high-spin and low-spin complexes,[11] obtaining the correct ground state represents a major challenge since GGA (generalized gradient approximation) functionals (e.g., PBE) tend to favor the low-spin states, while the hybrid functionals (e.g., B3LYP) artificially favor the high-spin states. Reiher related this behavior to the amount of exact Hartree−Fock exchange used in the hybrid functionals.[17] While it is difficult to accurately determine the ground state of spin crossover complexes or the exact energy differences between their high-spin and low-spin states with DFT methods, it is at

Received: October 29, 2011
Published: May 23, 2012

   dx.doi.org/10.1021/ic202344w | Inorg. Chem. 2012, 51, 6011−6019

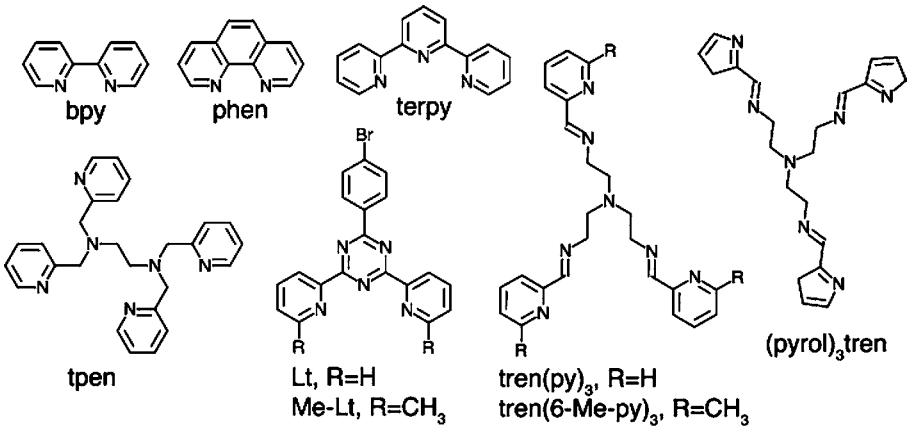

Figure 1. Heteropyridine ligands considered in this study.

least possible to qualitatively predict the effect of ligand substitution on the spin transition behavior.[12,15,16]

A number of different approaches were explored in order to alleviate the deficiencies of DFT in calculating the ground state of iron pseudo-octahedral complexes. For example, Reiher and co-workers suggested a reparametrization of the B3LYP functional resulting in the B3LYP* functional with reduced admixture of the Hartree−Fock (HF) exchange.[18,19,23] On the other hand, Pierloot and Vancoillie argued that while B3LYP* reparametrization performs considerably better than B3LYP for molecules with covalent bonds, one would need to increase the amount of Hartree−Fock exchange in the functional to properly describe the ionic complexes of iron and suggest CASPT2 as a more accurate methodology to study bonding and spin state energetics in the first row transition metal complexes.[24] More recently, Hughes and Friesner suggested a correction scheme to the B3LYP functional applicable to a broad set of first row transition metal compounds, containing both covalent and ionic complexes.[25] The M06-L functional[26,27] has also been shown to provide superior results for spin crossover complexes than B3LYP.

Here, we provide another insight into the applicability of the B3LYP functional to the ground state determination of pseudo-octahedral complexes of first row transition metals, with special focus on Fe(II) polypyridines. We confirm systematic trends in the calculated energy differences between the high-spin and low-spin electronic states observed previously[18] for a series of experimentally known transition metal complexes. Finally, we suggest that the ground state of an arbitrary Fe(II) complex can be determined by comparing the calculated energy difference between the low-spin and high-spin electronic states to the energy differences of structurally related complexes with a known, experimentally determined ground state, without the need to reparametrize the functional.

2. METHODOLOGY

We investigate 27 pseudo-octahedral complexes of Fe, Co, Mn, Ru, and Os with a mixture of heteropyridine and Cl^-, F^-, CN^-, NCS^-, NH_3, and H_2O ligands. The majority of the complexes (19) are complexes of iron. Heteropyridine ligands considered are shown in Figure 1. They include bpy = 2,2′-bipyridine, phen = 1,10-phenanthroline, terpy = 2,2′;6′,2″-terpyridine, tren(py)$_3$ = tris((N-(2-pyridylmethyl)-2-iminoethyl)amine), tren(6-Me-py)$_3$ = tris((N-(2-(6-Me-pyridyl)methyl)-2-iminoethyl)amine), Lt = 4-(4-bromophenyl)-2,6-bis(2-pyridine)-1,3,5-triazine, Me-Lt = 4-(4-bromophenyl)-2,6-bis(6-picolinyl)-1,3,5-triazine, tpen = tetrakis(2-pyridylmethyl)-ethylenediamine, and (pyrol)$_3$tren = tris(1-(2-azoyl)-2-azabuten-4-yl)amine ligands.

Geometries of all compounds were initially optimized at the B3LYP level of theory.[23] The SDD relativistic effective core potential and associated triple-ζ basis set[28] were used to describe the metal center, and the 6-311+G* basis set[29,30] was used for all other atoms. An ultrafine integration grid was used in all calculations. Singlet and quintet states were optimized for complexes of Fe(II), Co(III), Ru(II), and Os(II). Doublet and sextet states were optimized for complexes of Fe(III) and Co(II). Triplet and quintet states were optimized for the Mn(III) complex. All species were optimized both in a vacuum and solvent (water) using the Polarizable Continuum Model (PCM).[31] The use of solvent considerably improved the structures and spin contamination of small anionic species (e.g., $[Fe(CN)_6]^{4-}$) as well as improved or did not significantly change the geometries of neutral and cationic complexes. Due to its large size, $[Fe(Me\text{-}Lt)_2]^{2+}$ was optimized in a vacuum only, and single point calculations with PCM at the vacuum-optimized geometry were used to obtain the solvent corrections. All calculations were performed using the Gaussian 09 software package.[32]

To investigate the dependence of high-spin vs low-spin energy differences ($\Delta E_{HS/LS} = E_{high\text{-}spin} - E_{low\text{-}spin}$, $\Delta H_{HS/LS} = H_{high\text{-}spin} - H_{low\text{-}spin}$, $\Delta G_{HS/LS} = G_{high\text{-}spin} - G_{low\text{-}spin}$) on the amount of exact exchange in the B3LYP functional, we have systematically varied the c_1 parameter from 0.0 to 0.25, corresponding to 0−25% Hartree−Fock exchange in the exchange-correlation functional of B3LYP:

$$E_{xc} = E_{xc}^{LSDA} + c_1(E_x^{exact} - E_x^{LSDA}) + c_2\Delta E_x^{B88} + c_3\Delta E_C^{PW91} \quad (1)$$

in which c_1, c_2, and c_3 are coefficients fit from experimental data (determined to be $c_1 = 0.20$, $c_2 = 0.72$, $c_3 = 0.81$),[23] E_{xc}^{LSDA} is the exchange-correlation energy from the local spin density approximation (LSDA),[33] E_x^{exact} is the exact exchange energy, E_x^{B88} is Becke's 1988 gradient correction of exchange,[34] and ΔE_C^{PE91} is Perdew and Wang's 1991 gradient correction to correlation.[35]

Other functional forms, such as BHandHLYP,[36] BPW91,[34,35,37] B3PW91,[23,35,38] PBE,[39,40] and PBE0,[41] along with the Hartree−Fock calculations, were also used to investigate trends in the high-spin vs low-spin energy splitting for $[Fe(bpy)_2(NCS)_2)]^0$. The low-spin and high-spin geometries of all compounds were fully reoptimized at every level of theory considered, as well as for each different value of the exact exchange in the B3LYP functional. All optimized structures were verified using vibrational frequency analysis. The results of vibrational analysis were used to obtain enthalpies (H) and free energies (G) for all compounds at 298.15 K and standard pressure. An ultrafine integration grid was used for all calculations.

Calculated expectation values of the S^2 operator are within 10% of the value expected for each complex, except for the doublet spin-state of $[FeF_6]^{3-}$ ($\langle S^2\rangle = 1.79$ in vacuum and $\langle S^2\rangle = 1.14$ in water) and $[FeCl_6]^{3-}$ ($\langle S^2\rangle = 1.67$ in vacuum and $\langle S^2\rangle = 1.30$ in water). The S^2 expectation values are reported in the Supporting Information for all

dx.doi.org/10.1021/ic202344w | Inorg. Chem. 2012, 51, 6011−6019

complexes along with their Cartesian coordinates. The resulting wave functions were also tested for stability.[42,43]

3. RESULTS AND DISCUSSION

The aim of this work is to determine if the systematic behavior of high-spin vs low-spin energy differences with respect to the exact exchange admixture in the B3LYP functional can be used to obtain a ground state of Fe(II) polypyridine complexes without the need to reparametrize the hybrid functional. This relies on several assumptions. First, we assume that B3LYP is reliable in predicting the optimal geometries of high-spin as well as low-spin states of transition metal compounds. Second, in order for this approach to be reliable, we need to understand its limitations and be capable of identifying the cases in which it will work, as well as those in which it will not apply.

In this section, we start by examining the capability of the B3LYP to predict accurate geometries for a variety of high-spin and low-spin transition metal complexes by comparing the calculated geometries to crystal structure data available in the literature. Next, we confirm the relationship between the amount of exact exchange in the B3LYP functional (c_1) and high-spin vs low-spin energy splitting ($\Delta E_{HS/LS}$ and $\Delta G_{HS/LS}$).[18,19] We further show that the dependence of $\Delta E_{HS/LS}$ (as well as $\Delta G_{HS/LS}$) on c_1 is closely related to the identity of transition metal ligands and, in turn, to the average change in the metal−ligand bond lengths between the low-spin and high-spin states. We also show that for a set of structurally related complexes, the error in $\Delta E_{HS/LS}$ is systematic and correctly reflects relative stabilities of high-spin vs low-spin states. This observation allows us to come up with a practical way to determine the ground state of an unknown complex by comparing its calculated $\Delta E_{HS/LS}$ to the $\Delta E_{HS/LS}$ for a set of structurally related, experimentally known complexes.

3.1. Ground State Geometries of Fe(II) Polypyridine Complexes. We used density functional theory at the B3LYP level to obtain high-spin and low-spin geometries of several transition metal complexes with a general formula $M(L)_x(L')_y$, where $x = 0-3$; $y = 0, 2, 4, 6$; L = bpy, phen, terpy, tren(py)$_3$, tren(6-Me-py)$_3$, (pyrol)$_3$tren, tpen, Lt, and Me-Lt; and L′ = CN^-, NCS^-, F^-, Cl^-, H_2O, and NH_3. Since the pseudo-octahedral environment around the central atom is the most critical in determining the properties of these compounds, we have compared metal−donor atom bond lengths (donor atoms: C, N, O, F, and Cl) obtained from the geometry optimization with the B3LYP functional to the bond lengths from the corresponding crystal structures. Note that only 22 out of 25 first-row transition metal complexes investigated in this work have available crystal structure data in the literature. The results are summarized in Table 1.

The B3LYP geometries for the octahedral coordination environment of all complexes investigated are under 5% average error in metal−ligand bond length of corresponding ground state crystal structures. The average error in the optimized geometries of anionic, neutral, and cationic species in a vacuum was 4.6, 3.1, and 3.3%, respectively; in a solvent, we find these average errors for anionic, neutral, and cationic species to be 2.6, 2.3, and 3.0%, respectively. The use of a solvent most significantly improves the geometries of the anionic species and in particular the species with six ligands derived from small anions (F^-, Cl^-, CN^-). The results show that the B3LYP functional is able to accurately predict geometries for the transition metal complexes of interest and would provide good predictive power for unknown complexes if the correct ground state could be determined.

Table 1. Percent Errors in Metal−Ligand Bond Lengths Obtained from the B3LYP Optimized Geometries with Respect to Crystal Structure Data of First Row Transition Metal Complexes Studied

complex (spin multiplicity)[a]	% error (M−L)	complex (spin multiplicity)[a]	% error (M−L)
$[Fe(bpy)_2(CN)_2]^0$ (singlet)	2.4	$[Fe(terpy)_2]^{2+}$ (singlet)	2.7
$[Fe(bpy)(CN)_4]^{2-}$ (singlet)	2.4	$[Fe(tren(py)_3)]^{2+}$ (singlet)	2.9
$[Fe(CN)_6]^{4-}$ (singlet)	2.6	$[Fe(tren(6\text{-}Me\text{-}py)_3)]^{2+}$ (quintet)	4.0
$[Fe(bpy)_2(NCS)_2]^0$ (singlet)	2.3	$[FeF_6]^{3-}$ (sextet)	3.4
$[Fe(bpy)_2Cl_2]^0$ (quintet)	3.4	$[FeCl_6]^{3-}$ (sextet)	3.0
$[Fe(bpy)_3]^{2+}$ (singlet)	3.1	$[Fe(pyrol)_3tren]^0$ (doublet)	1.7
$[Fe(phen)_3]^{2+}$ (singlet)	2.9	$[Mn(pyrol)_3tren]^0$ (doublet)	1.5
$[Fe(Lt)_2]^{2+}$ (singlet)	3.0	$[Co(bpy)_3]^{2+}$ (quartet)	2.2
$[Fe(Me\text{-}Lt)_2]^{2+}$ (quintet)	2.6[b]	$[Co(terpy)_2]^{2+}$ (doublet)	4.3
$[Fe(tpen)]^{2+}$ (singlet)	2.8	$[Co(CN)_6]^{3-}$ (singlet)	1.6
$[Fe(H_2O)_6]^{2+}$ (quintet)	4.0	$[Co(NH_3)_6]^{3+}$ (singlet)	1.6
average % error: 2.7			

[a]Experimental ground states obtained from references 44−64. [b]All compounds were optimized in water using the PCM, while $[Fe(Me\text{-}Lt)_2]^{2+}$ was optimized in vacuum.

3.2. Ground State Determination by B3LYP, Energies of High-Spin vs Low-Spin States. While B3LYP can be used as a reliable tool in obtaining high-spin and low-spin geometries of first row transition metal complexes, it is not as reliable in predicting their ground state spin multiplicity. Out of the 25 first row transition metal complexes investigated, B3LYP was incorrect in predicting the ground state of eight of these, artificially favoring the high-spin state over the low-spin state in seven of the cases (see Table 2). The inclusion of thermal and entropic factors further stabilized the high-spin state in four more complexes and incorrectly predicted the high-spin ground state for 10 of the 25 complexes. Such bias toward the high-spin states is not unusual for the B3LYP and has been observed before.[18]

Following the example of Reiher et al.,[18] we have calculated the energy ($\Delta E_{HS/LS}$), as well as enthalpy ($\Delta H_{HS/LS}$) and free energy differences ($\Delta G_{HS/LS}$) between the high-spin and low-spin states for a group of transition metal compounds with respect to the exact exchange admixture in the B3LYP functional form (c_1 = 0.00−0.25, see eq 1). The energy difference was defined as $\Delta E_{HS/LS} = E_{high\text{-}spin} - E_{low\text{-}spin}$ ($\Delta H_{HS/LS} = H_{high\text{-}spin} - H_{low\text{-}spin}$, $\Delta G_{HS/LS} = G_{high\text{-}spin} - G_{low\text{-}spin}$) and is positive if the low-spin state is calculated to be more stable than the high-spin state.

Figure 2 shows the $\Delta E_{HS/LS}$ dependence on c_1 for a number of different Fe(II) pseudo-octahedral complexes with polypyridine as well as nonpolypyridine ligands both in a vacuum (dashed line) and in water (solid line). While $\Delta E_{HS/LS}$ depends linearly on c_1, the slope of this dependence varies widely among the complexes, and it is not possible to fit this dependence with

dx.doi.org/10.1021/ic202344w | Inorg. Chem. 2012, 51, 6011−6019

Table 2. Experimental and Calculated (B3LYP/SDD, 6-311+G*) Ground State Spin Multiplicities of Pseudo-Octahedral First Row Transition Metal Complexes Investigated in This Work

complex	experimental	calculated from $\Delta E_{HS/LS}$	calculated from $\Delta G_{HS/LS}$
$[Fe(bpy)_2(CN)_2]^0$	singlet[65]	singlet	quintet
$[Fe(bpy)(CN)_4]^{2-}$	singlet[65]	singlet	singlet
$[Fe(CN)_6]^{4-}$	singlet[66]	singlet	singlet
$[Fe(bpy)_2(NCS)_2]^0$	singlet[a,50]	quintet	quintet
$[Fe(bpy)_2Cl_2]^0$	quintet[52]	quintet	quintet
$[Fe(bpy)_3]^{2+}$	singlet[66]	singlet	quintet
$[Fe(phen)_3]^{2+}$	singlet[66]	quintet	quintet
$[Fe(Lt)_2]^{2+}$	singlet[58]	quintet	quintet
$[Fe(Me\text{-}Lt)_2]^{2+}$	quintet[58]	quintet	quintet
$[Fe(tpen)]^{2+}$	singlet[a,61]	quintet	quintet
$[Fe(terpy)_2]^{2+}$	singlet[67]	quintet	quintet
$[Fe(tren(py)_3)]^{2+}$	singlet[68]	quintet	quintet
$[Fe(tren(6\text{-}Me\text{-}py)_3)]^{2+}$	quintet[68]	quintet	quintet
$[Fe(H_2O)_6]^{2+}$	quintet[66]	quintet	quintet
$[Fe(NH_3)_6]^{2+}$	quintet[69]	quintet	quintet
$[Fe(NH_3)_6]^{3+}$	sextet[69]	doublet	sextet
$[FeF_6]^{3-}$	sextet[70]	sextet	sextet
$[FeCl_6]^{3-}$	sextet[53]	sextet	sextet
$[Fe(pyrol)_3tren]^0$	doublet[55]	doublet	sextet
$[Mn(pyrol)_3tren]^0$	quintet[57]	quintet	quintet
$[Co(bpy)_3]^{2+}$	quartet[71]	quartet	quartet
$[Co(terpy)_2]^{2+}$	doublet[a,72]	quartet	quartet
$[CoF_6]^{3-}$	quintet[73]	quintet	quintet
$[Co(CN)_6]^{3-}$	singlet[62]	singlet	singlet
$[Co(NH_3)_6]^{3+}$	singlet[64]	singlet	singlet

[a]Denotes thermal spin crossover complexes.

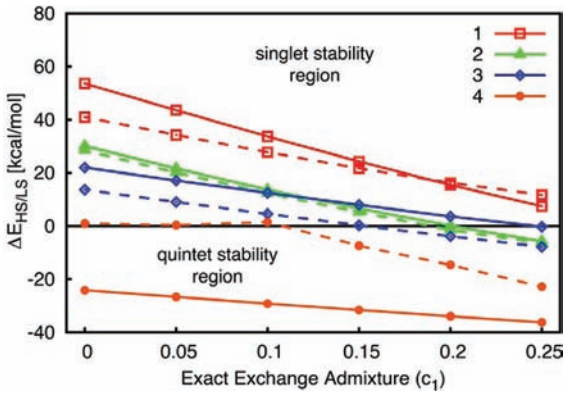

Figure 2. Dependence of the energy difference, $\Delta E_{HS/LS} = E_{high\text{-}spin} - E_{low\text{-}spin}$ (kcal/mol), on the exact exchange admixture (c_1) in the B3LYP functional for iron pseudo-octahedral complexes with various ligands: $[Fe(bpy)(CN)_4]^{2-}$ (**1**), $[Fe(bpy)_3]^{2+}$ (**2**), $[Fe(NH_3)_6]^{3+}$ (**3**), $[FeF_6]^{3-}$ (**4**). $\Delta E_{HS/LS} > 0$ corresponds to the low-spin ground state (singlet or doublet); $\Delta E_{HS/LS} < 0$ corresponds to the high-spin ground state (quintet or sextet). Solid lines are calculated in a solvent (water, PCM); dashed lines are calculated in a vacuum.

a single linear equation for all complexes investigated. Similar behavior was reported previously by Salomon et al.[19] for a different set of first row transition metal complexes.

Figure 2 also demonstrates how the dependence of $\Delta E_{HS/LS}$ on c_1 is influenced by the inclusion of solvent (water) via the PCM. A majority of the complexes investigated display behavior that is quite insensitive toward the solvent inclusion via the PCM and behave similarly to $[Fe(bpy)_3]^{2+}$ (complex 2 in Figure 2). A small number of complexes, mostly those that are negatively charged, undergo a remarkable change in their behavior when the calculations are performed in a solvent. For example, $[FeF_6]^{3-}$ (complex 4 in Figure 2) displays nonlinear behavior in its dependence of $\Delta E_{HS/LS}$ on c_1 when optimizations are performed in a vacuum. Further investigation of this phenomenon revealed the presence of two different high-spin states for this complex, whose relative stabilities change depending on the amount of exact exchange in the B3LYP functional. Therefore, calculations performed with a lower admixture of exact exchange converge to a different electronic state than those with a higher admixture, resulting in the nonlinear behavior. This problem of state switching for $[FeF_6]^{3-}$ is not present when optimizations are performed in solvent (water) using PCM, as the inclusion of the PCM results in the stabilization of a different electronic state.

Table 3 summarizes the behavior of all complexes investigated, giving the slope of the linear fit for the dependence of $\Delta E_{HS/LS}$, $\Delta H_{HS/LS}$, and $\Delta G_{HS/LS}$ on the amount of exact exchange (c_1). The plots of $\Delta H_{HS/LS}$ and $\Delta G_{HS/LS}$ vs c_1 for all complexes investigated can be found in the Supporting Information.

Interestingly, all Fe(II) polypyridine complexes have a similar slope of ΔE vs c_1 across the 0.0−0.25 range of the exact exchange admixture. On the other hand, while the dependence of ΔE vs c_1 for more ionic complexes (e.g., $[Fe(H_2O)]^{2+}$, $[FeCl_6]^{4-}$) is still linear, the slope of this dependence is completely different from that of the Fe(II) polypyridine compounds. This makes it challenging to come up with a single correction scheme for a wide variety of transition metal compounds. We suggest that there is a connection between the slope of the ΔE vs c_1 dependence and structural features of the complexes, as well as the character of metal−ligand bonds in the complex (ionic vs covalent).

3.3. Structure of Fe(II) Complexes and Error in High-Spin/Low-Spin Energies from B3LYP. According to ligand field theory, the ligand field splitting between a set of t_{2g} and e_g metal orbitals is determined by the identity of a central atom and its ligands. The size of the ligand field splitting determines the ground state electronic configuration (high-spin vs low-spin) as well as the energy difference between the high-spin/low-spin states of a particular octahedral compound. Therefore, it would not be surprising if there were some link between the structure of the complexes investigated and the slope of $\Delta E_{HS/LS}$ vs c_1.

The change in the electronic configuration from high-spin to low-spin and vice versa is usually accompanied by a marked change in the metal−ligand bond lengths of the covalent complexes, as placing the electrons into the antibonding e_g orbitals increases the metal−ligand distance in the high-spin state. Therefore, we have explored the relationship between the average change in the metal−ligand distance (ΔR) and the slope of the $\Delta E_{HS/LS}$ dependence on the amount of exact exchange in the B3LYP functional (c_1). The reported ΔR is an average over the c_1 range investigated, but the results are virtually identical when only considering ΔR calculated at c_1 = 0.2 (unmodified B3LYP functional).

Table 3 summarizes the average change in the metal−ligand distance between the high-spin and low-spin states determined at the B3LYP level of theory along with the slope of the $\Delta E_{HS/LS}$, $\Delta H_{HS/LS}$, and $\Delta G_{HS/LS}$ dependence on c_1. The change in the metal−ligand distance was determined as an average of

dx.doi.org/10.1021/ic202344w | Inorg. Chem. 2012, 51, 6011−6019

Table 3. Table of Average Change in Metal−Ligand Bond Lengths ΔR(metal−ligand) in Ångstroms for Low-Spin to High-Spin Transition versus Slope of the Scan over the Exact Exchange for Various Pseudo-Octahedral Complexes

complex	ΔR (metal−ligand) [Å]	slope of scan $d(\Delta E)/dc_1$	slope of scan $d(\Delta H)/dc_1$	slope of scan $d(\Delta G)/dc_1$
$[Fe(CN)_6]^{4-}$	0.3336	−214.17	−212.51	−208.92
$[Fe(bpy)(CN)_4]^{2-}$	0.2726	−185.56	−184.48	−181.69
$[Fe(bpy)_2(CN)_2]^0$	0.2337	−161.42	−160.73	160.02
$[Co(CN)_6]^{3-}$	0.2295	−145.62	−143.93	−137.59
$[Fe(Lt)_2]^{2+}$	0.2266	−160.18	−158.10	−161.41
$[Fe(tren(py)_3)]^{2+}$	0.2265	−147.79	−146.01	−141.98
$[Fe(terpy)_2]^{2+}$	0.2149	−156.18	−154.86	−152.45
$[Fe(tren(6\text{-}Me\text{-}py)_3)]^{2+}$	0.2125	−142.97	−141.98	−142.88
$[Fe(tpen)]^{2+}$	0.2044	−125.25	−124.52	−117.40
$[Fe(bpy)_3]^{2+}$	0.2013	−143.56	−143.20	−141.62
$[Fe(bpy)_2(NCS)_2]^0$	0.2003	−125.76	−124.30	−124.48
$[Fe(phen)_3]^{2+}$	0.1994	−139.34	−139.67	−138.29
$[Fe(Me\text{-}Lt)_2]^{2+}$	0.1991	−142.16	−149.73	−156.79
$[Fe(NH_3)_6]^{2+}$	0.1827	−91.95	−92.05	−90.70
$[Fe(bpy)_2Cl_2]^0$	0.1755	−126.90	−127.05	−127.54
$[Fe(pyrol)_3tren]^0$	0.1655	−97.80	−96.84	−92.48
$[Co(NH_3)_6]^{3+}$	0.1561	−88.39	−90.37	−93.56
$[Fe(NH_3)_6]^{3+}$	0.1498	−89.33	−92.26	−93.07
$[Co(bpy)_3]^{2+}$	0.1290	−89.33	−89.55	−87.59
$[Fe(H_2O)_6]^{2+}$	0.1230	−62.12	−62.24	−63.08
$[Co(terpy)_2]^{2+}$	0.1136	−93.29	−90.49	−97.06
$[Mn(pyrol)_3tren]^0$	0.1095	−58.44	−58.88	−57.12
$[FeCl_6]^{3-}$	0.0908	−54.97	−54.51	−49.97
$[CoF_6]^{3-}$	0.0638	−45.42	−38.17	−30.97
$[FeF_6]^{3-}$	0.0610	−48.25	−47.47	−42.93
$[Ru(bpy)_3]^{2+}$	0.2760	−109.44	−108.74	−112.39
$[Os(bpy)_3]^{2+}$	0.1372	−16.74[a]	−9.21[a]	−17.89[a]

[a] $[Os(bpy)_3]^{2+}$ quintet changes electronic states over the exact exchange admixture investigated.

the changes calculated for all values of c_1 investigated between 0.0 and 0.25. Figure 3 shows the plot of the average change in

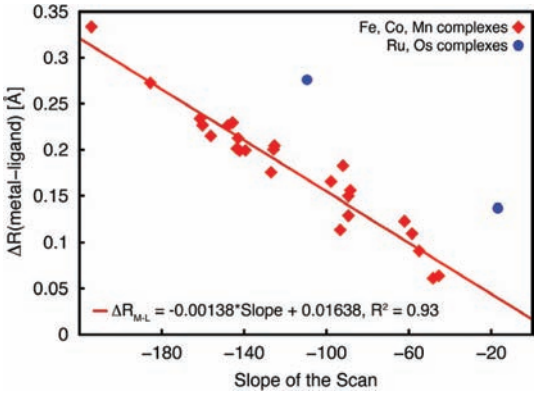

Figure 3. Plot of the average change in metal to ligand bond lengths in transition from low-spin to high-spin states versus the slope of the scan over exact exchange for data shown in Table 3 along with a plot of the linear regression, $R^2 = 0.93$.

the metal−ligand bond lengths between the high-spin and low-spin states, with respect to the slope of the $\Delta E_{HS/LS}$ vs c_1 dependence. Interestingly, there is a linear relationship between the two, showing that a smaller slope corresponds to a smaller change in the bond lengths. The R^2 coefficient for this dependence is 0.93, suggesting a strong correlation. Second and third-row transition metal compounds ($[Ru(bpy)_3]^{2+}$, $[Os(bpy)_3]^{2+}$, shown in blue) were excluded from the fit, but are still shown on the plot. A weaker correlation is observed, with an R^2 value of 0.78, when all species are optimized in a vacuum (provided in the Supporting Information). All species reported in Table 3 were optimized using the PCM solvent model for water, excluding $[Fe(Me\text{-}Lt)_2]^{2+}$, for which solvent corrections are included via a single point calculation at the vacuum-optimized geometry.

It is apparent that the complexes with the weakest dependence of $\Delta E_{HS/LS}$ on c_1 are ionic compounds of first row transition metals (e.g., $[FeF_6]^{3-}$, $[FeCl_6]^{3-}$) that also undergo the smallest change in the metal−ligand bond lengths between the low-spin and high-spin states. Complexes with more covalent character of metal−ligand bonds undergo larger structural changes between their low-spin and high-spin electronic states and are more strongly influenced by the amount of exact exchange admixture in the DFT functional.

The outliers to this trend are shown in blue and belong to octahedral compounds with a central atom from the second and third rows of transition metals (Ru and Os), suggesting that the relationship between the average change in metal−ligand bond lengths and the slope of the $\Delta E_{HS/LS}$ dependence on c_1 will have a different character than displayed by the complexes of first row transition metals.

Note that a similar relationship as observed between the dependence of $\Delta E_{HS/LS}$ on c_1 vs ΔR holds true for $\Delta H_{HS/LS}$ and $\Delta G_{HS/LS}$. The correlation for this dependence becomes slightly worse with the thermal and entropic corrections included (R^2 = 0.93 and 0.91, respectively). This is not very surprising, as several assumptions are made in obtaining these corrections (i.e., assumption of harmonic potential, neglecting the role of

dx.doi.org/10.1021/ic202344w | Inorg. Chem. 2012, 51, 6011−6019

the solvent) that are not equally good for all compounds investigated in this study. The problem is exacerbated by the fact that the low frequency vibrations, which provide the largest contribution to the entropy, suffer from the highest error in the harmonic approximation.[17]

It is also important to mention that the changes in the enthalpies and Gibbs free energies ($\Delta H_{HS/LS}$, $\Delta G_{HS/LS}$) reported here are effectively the changes in the gas-phase enthalpies and Gibbs free energies corrected for the solvent effects implicitly via the use of the PCM. In reality, the low-spin to high-spin transition is a condensed-phase phenomenon with important entropic contributions originating in electronic, vibrational, rotational, and phonon (intermolecular) degrees of freedom. The major contribution to the entropy change (and, therefore, $\Delta G_{HS/LS}$) arises from the geometrical changes that complexes undergo upon their transition between the high-spin and low-spin states. This can be extracted from calculated vibrational spectra of both high-spin and low-spin states, which was done in the present work. Optical phonons (not included in our model) will also provide a significant contribution to the entropy change.[74] An in-depth analysis of these and related issues for the correct determination of $\Delta G_{HS/LS}$ is provided in the work of Brehm and co-workers.[74,75]

It is also worth mentioning that essentially the same results are obtained when the analysis is performed with a smaller basis set (6-31G* instead of 6-311+G*) and in a vacuum. The larger basis set and solvent model are, however, necessary to obtain a proper description of the structures and electronic states of some anionic compounds, especially $[Fe(CN)_6]^{4-}$ and $[FeF_6]^{3-}$.

3.4. Ground State Determination for a Family of Structurally Related Complexes. The linear correlation between the average ΔR and slope of the $\Delta E_{HS/LS}$ vs c_1 suggests that the octahedral complexes that undergo similar distortion in their octahedral environment going from a low-spin to high-spin state (described here by the average change in metal–ligand bond lengths) suffer from a similar error in the B3LYP functional. In the case of the covalent complexes of iron, this systematic error results in the artificial stabilization of their high-spin state energies with respect to the low-spin state energies. The question still remains if this error is systematic for a group of similar complexes, i.e., if it results in the artificial stabilization of the high-spin state energies with respect to the low-spin state energies by about the same amount.

To find whether the error is indeed systematic, we have looked at the $\Delta E_{HS/LS}$ vs c_1 dependence in a set of 11 structurally related Fe(II) polypyridine complexes. They were chosen as "structurally related" because they display a similar geometry change in the metal–ligand bond lengths going from low-spin to high-spin geometry (see Table 3). The selected complexes contain polypyridine ligands combined with other ligands of varying ligand-field strengths, such as Cl^-, NCS^-, and CN^-. The plot of the $\Delta E_{HS/LS}$ as a function of c_1 for six members from this family of related Fe(II) compounds is shown in Figure 4.

As can be seen in Figure 4, the dependence of $\Delta E_{HS/LS}$ on c_1 is linear, with approximately the same slope for the compounds considered. Note that very similar linear dependence of $\Delta E_{HS/LS}$ on c_1 as well as systematic errors for a group of related Fe(II)–S complexes have been observed previously by Reiher and co-workers.[18] In the case of our Fe(II) test complexes, this linear relationship between ΔE and c_1 can be described by the following equation:

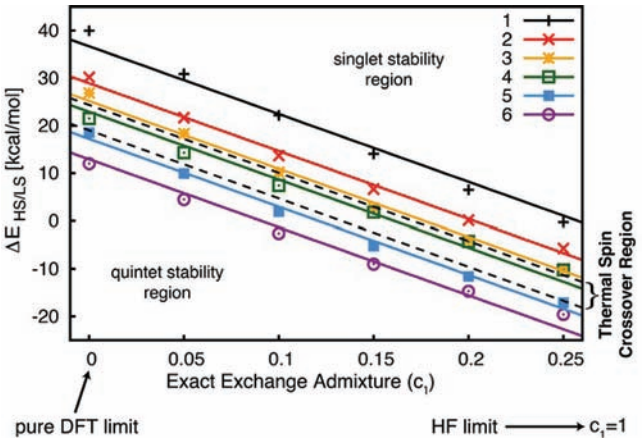

Figure 4. Dependence of the energy difference, $\Delta E_{HS/LS} = E_{high\text{-}spin} - E_{low\text{-}spin}$ (kcal/mol), on the exact exchange admixture (c_1) in the B3LYP functional for several pseudo-octahedral iron(II) polypyridine complexes: $[Fe(bpy)_2(CN)_2]^0$ (**1**), $[Fe(bpy)_3]^{2+}$ (**2**), $[Fe(tren(py)_3)]^{2+}$ (**3**), $[Fe(bpy)_2(NCS)_2]^0$ (**4**), $[Fe(tren(6\text{-Me-}py)_3)]^{2+}$ (**5**), and $[Fe(bpy)_2Cl_2]^0$ (**6**). $\Delta E_{HS/LS} > 0$ corresponds to the singlet ground state; $\Delta E_{HS/LS} < 0$ corresponds to the quintet ground state. A linear regression is plotted for each complex based on the constant slope formula $\Delta E_{HS/LS} = I - 142.5c_1$.

$$\Delta E_{HS/LS} = I - 142.5c_1 \quad (2)$$

where I corresponds to the intercept (the value of $\Delta E_{HS/LS}$ at $c_1 = 0$ for each complex) which describes the vertical shift between the plots of $\Delta E_{HS/LS}$ vs c_1 for different complexes. The five complexes included in the fit but not shown in Figure 4 are $[Fe(Lt)_2]^{2+}$, $[Fe(Me\text{-}Lt)_2]^{2+}$, $[Fe(phen)_3]^{2+}$, $[Fe(terpy)_2]^{2+}$, and $[Fe(tpen)]^{2+}$. The above equation fits the $\Delta E_{HS/LS}$ dependence on c_1 for each of the 11 complexes very accurately, with the correlation coefficient $R^2 = 0.97–0.99$. More importantly, the vertical shift between plots of $\Delta E_{HS/LS}$ for different Fe(II) compounds correctly reflects the change in the ligand field strength of their ligands, meaning that the low-spin states of Fe(II) compounds are stabilized over the high-spin states in the same order as the Fe(II) ligands appear in the spectrochemical series: Cl^- < NCS^- < pyridine < bipyridine < CN^-. This means that although B3LYP is not capable of predicting the correct ground state spin multiplicities, the overall order of the high-spin/low-spin energy differences for a group of structurally related compounds reflects their high-spin, low-spin, or thermal spin crossover character in the ground state.

It should be noted that when comparing $[Fe(phen)_3]^{2+}$ and $[Fe(bpy)_3]^{2+}$ we found that the trend in $\Delta E_{HS/LS}$ vs c_1 incorrectly reflected the trend in ligand field strength; however, the distance between the two plots of $\Delta E_{HS/LS}$ over $c_1 = 0–0.25$ was at most 2.0 kcal/mol. $[Fe(phen)_3]^{2+}$ is not shown in Figure 4 but belongs to the same set of structurally related complexes. Phen and bpy ligands are considered to have very similar ligand field strengths, so this discrepancy is well within the accepted error range for the B3LYP functional.

The linear behavior of $\Delta E_{HS/LS}$ with respect to c_1, along with the systematic trend in the intercept I for a series of related compounds, can therefore be used to construct a benchmark for determination of the ground state multiplicity for an arbitrary Fe(II) polypyridine complex. A procedure to determine the ground state multiplicity of an arbitrary Fe(II) polypyridine complex could be as follows: (1) Obtain $\Delta E_{HS/LS}$

dx.doi.org/10.1021/ic202344w | Inorg. Chem. 2012, 51, 6011–6019

vs exact exchange dependence plots for a series of related compounds with available experimental reference data. (2) On the basis of this benchmark, decide which values of the intercept I correspond to the high-spin and low-spin ground states. In the specific example of Fe(II) polypiridines shown in Figure 4, I > 24 kcal/mol indicates a low-spin complex, I < 18 kcal/mol high-spin complex, with I = 18−24 kcal/mol indicating a possible thermal spin crossover complex. (3) Obtain $\Delta E_{HS/LS}$ vs exact exchange dependence plot for the compound with unknown ground state. (4) On the basis of the intercept I obtained for the unknown compound, determine its spin state.

For a series of related complexes, this procedure will produce a unique range of I values describing the regions of low-spin and high-spin stability. A spin crossover region will also always exist between the two stability regions due to the inherent uncertainty of the method. The value of the intercept I obtained for a thermal spin crossover complex determines a "critical value", i.e., the value at which the change between the low-spin and high-spin regions occurs. In the particular case presented here, the average value of the intercepts I calculated for two thermal spin crossover complexes included in the analysis ($[Fe(tpen)]^{2+}$, $[Fe(bpy)_2(NCS)_2]^0$) is 21 kcal/mol. Curiously, this value is virtually identical with the calculated value of the exchange interaction between electrons in the d orbitals of iron (20.1−20.9 kcal/mol).[76−78]

The strong linear correlation between the average ΔR and slope of the $\Delta E_{HS/LS}$ vs c_1 scans could also allow us to forego the calculation of $\Delta E_{HS/LS}$ vs c_1 dependence for several values of c_1 for both benchmark and unknown complexes. It makes it possible for us to rely on the average change in the octahedral coordination environment to determine what group of complexes is "similar" for the purposes of the ground state determination and reduces the number of calculations one needs to perform to just B3LYP with a single value of c_1 = 0.2. Analogous analysis with virtually identical results toward lower energies can also be performed using $\Delta H_{HS/LS}$ or $\Delta G_{HS/LS}$ instead of $\Delta E_{HS/LS}$, noting that the calculated $\Delta H_{HS/LS}$ and $\Delta G_{HS/LS}$ will be systematically shifted toward lower energies.

3.5. High-Spin/Low-Spin Energy Trends with Other Density Functionals. As a point of interest, it is worth noting that the trend established in the energy differences between the quintet and singlet states in iron(II) complexes applies more generally than to just the B3LYP functional. We used multiple density functionals (BHandHLYP,[36] BPW91,[34,35,37] B3PW91,[23,35,38] PBE,[39,40] and PBE0[41]) and Hartree−Fock calculations to determine the energy difference between the quintet and singlet states of $[Fe(bpy)_2(NCS)_2]^0$. The scatter plot of $\Delta E_{HS/LS}$ vs the amount of exact exchange in each of the functionals is shown in Figure 5. First, the slope of $\Delta E_{HS/LS}$ vs the amount of exact exchange in B3LYP is not linear over the entire range of the exact exchange admixture. This is consistent with the findings reported previously by Salomon et al.[19] More importantly, other DFT functionals closely follow the same trend as the modified B3LYP, suggesting that the major error in the energy difference between the high-spin and low-spin states arises from the contribution of exact exchange, and similar correction schemes as used with the B3LYP functional can be applied with other functionals as well.

4. CONCLUSIONS

In this work, we investigated the applicability of the B3LYP functional to accurate prediction of ground state multiplicity of

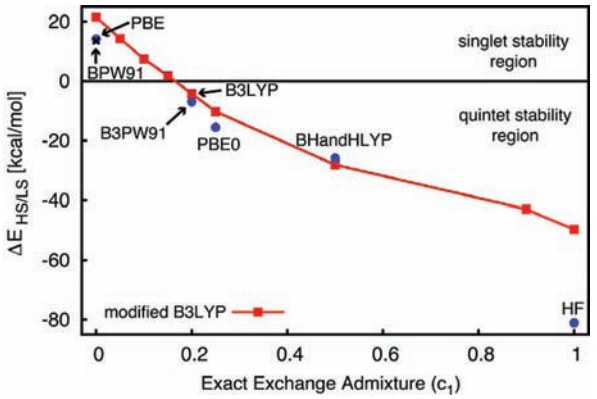

Figure 5. Plot of energy difference, $\Delta E_{HS/LS}$ (kcal/mol), calculated in water (PCM model) between quintet and singlet states of $[Fe(bpy)_2(NCS)_2)]^0$ versus the fraction of exact exchange in the B3LYP functional form (c_1 = 0.00 to 0.25), BHandHLYP (0.50 exact exchange), BPW91 (0.00 exact exchange), B3PW91 (0.20 exact exchange), PBE (0.00 exact exchange), and PBE0 (0.25 exact exchange) and pure Hartree−Fock calculation (1.0 exact exchange).

pseudo-octahedral iron complexes. Iron complexes are of great interest due to potential applications as molecular switches, data storage materials, and chromophores in dye-sensitized solar cells. Their properties intrinsically depend on their ground state, which, depending on the ligand character, can be either low-spin or high-spin. In general, density functional theory has difficulties with predicting the correct ground state multiplicity of such compounds, as pure functionals favor the low-spin states and hybrid functionals with a high fraction of exact Hartree−Fock exchange tend to favor high-spin ground states.

We confirmed the linear relationship between the high-spin/low-spin energy splitting, $\Delta E_{HS/LS}$ ($\Delta E_{HS/LS}$ = $E_{high\text{-}spin}$ − $E_{low\text{-}spin}$), as well as $\Delta H_{HS/LS}$ and $\Delta G_{HS/LS}$, and the amount of exact exchange in the B3LYP functional as previously observed by Reiher.[17] For coordination complexes of iron with mostly covalent character, such as Fe(II) polypyridines, $\Delta E_{HS/LS}$ displays a strong dependence on the amount of exact exchange in the functional, and B3LYP tends to favor high-spin ground states. On the other hand, $\Delta E_{HS/LS}$ for ionic complexes displays a weaker dependence on c_1, and B3LYP artificially stabilizes the low-spin states.

We confirmed that in most cases investigated, dependence of $\Delta E_{HS/LS}$ on c_1 is linear over the range of 0−25% of exact exchange admixture in modified B3LYP. We found that the slope of this dependence strongly correlates with the average change in the metal−ligand bond lengths between the low-spin and high-spin states. Moreover, the error in $\Delta E_{HS/LS}$ for a group of structurally related complexes (i.e., complexes that undergo similar change in the metal−ligand bond lengths between the high-spin and low-spin states) is systematic, and the calculated values of $\Delta E_{HS/LS}$ correctly reflect the trend in the relative stabilities of their low-spin and high-spin states. Inclusion of thermal and entropic corrections tends to stabilize the high-spin states but nevertheless results in identical behavior. This systematic behavior allows for a ground state determination of an arbitrary pseudo-octahedral complex of iron by comparing the calculated energy differences between the singlet and quintet electronic states of an unknown complex to the energy differences of structurally related complexes with a known, experimentally determined ground state.

dx.doi.org/10.1021/ic202344w | Inorg. Chem. 2012, 51, 6011−6019

■ ASSOCIATED CONTENT

Supporting Information

Plots of $\Delta E_{HS/LS}$, $\Delta H_{HS/LS}$, and $\Delta G_{HS/LS}$ in kcal/mol versus exact exchange admixture (c_1) in the B3LYP functional for all of the complexes investigated. Plots of ΔR versus the calculated slopes of $\Delta E_{HS/LS}$, $\Delta H_{HS/LS}$, and $\Delta G_{HS/LS}$ (kcal/mol) when scanning across exact exchange for all complexes, both in a vacuum and in water (PCM). Results of linear regression analysis for a set of 11 structurally related Fe(II) polypyridine complexes. Tables of high-spin and low-spin energy differences ($\Delta E_{HS/LS}$, $\Delta H_{HS/LS}$, and $\Delta G_{HS/LS}$ in kcal/mol) for different amounts of exact exchange in the B3LYP functional for all complexes investigated, including various DFT functionals and HF for the $[Fe(bpy)_2(NCS)_2]^0$ complex. Included is a list of Cartesian coordinates in Ångströms for high-spin and low-spin states of all complexes considered in this study optimized at the B3LYP level of theory along with calculated $\langle S^2 \rangle$ for open shell systems. This material is available free of charge via the Internet at http://pubs.acs.org.

■ AUTHOR INFORMATION

Corresponding Author

*E-mail: ejakubi@ncsu.edu.

Notes

The authors declare no competing financial interest.

■ ACKNOWLEDGMENTS

This research was supported by the U.S. Department Of Education Graduate Assistance In Areas Of National Need (GAANN) Fellowship Program at North Carolina State University (D.N.B.) and Army Research Office Grant 59842-CH-II (E.J.).

■ REFERENCES

(1) Létard, J. F.; Guionneau, P.; Goux-Capes, L. *Spin Crossover in Transition Metal Compounds III*; Springer: New York, 2004; Vol. *1*, pp 1−19.
(2) Gütlich, P.; Goodwin, H. A. *Spin Crossover in Transition Metal Compounds I*; Springer: New York, 2004; Vol. *1*, pp 1−47.
(3) Ferrere, S. *Chem. Mater.* **2000**, *12*, 1083−1089.
(4) Ferrere, S. *Inorg. Chim. Acta* **2002**, *329*, 79−92.
(5) Ferrere, S.; Gregg, B. A. *J. Am. Chem. Soc.* **1998**, *2*, 843−844.
(6) Yang, M.; Thompson, D. W.; Meyer, G. J. *Inorg. Chem.* **2000**, *39*, 3738−3739.
(7) Yang, M.; Thompson, D. W.; Meyer, G. J. *Inorg. Chem.* **2002**, *41*, 1254−1262.
(8) Monat, J. E.; McCusker, J. K. *J. Am. Chem. Soc.* **2000**, *122*, 4092−4097.
(9) Juban, E.; Smeigh, A.; Monat, J. *Coord. Chem. Rev.* **2006**, *250*, 1783−1791.
(10) Smeigh, A. L.; Creelman, M.; Mathies, R. a.; McCusker, J. K. *J. Am. Chem. Soc.* **2008**, *130*, 14105−14107.
(11) Lawson Daku, L. M.; Vargas, A.; Hauser, A.; Fouqueau, A.; Casida, M. E. *ChemPhysChem* **2005**, *6*, 1393−1410.
(12) Paulsen, H.; Duelund, L.; Winkler, H.; Toftlund, H.; Trautwein, A. X. *Inorg. Chem.* **2001**, *40*, 2201−2203.
(13) Shiota, Y.; Sato, D.; Juhasz, G.; Yoshizawa, K. *J. Phys. Chem. A* **2010**, *114*, 5862−5869.
(14) Zein, S.; Matouzenko, G. S.; Borshch, S. A. *J. Phys. Chem. A* **2005**, *109*, 8568−8571.
(15) Paulsen, H.; Trautwein, A. *Spin Crossover in Transition Metal Compounds III*; Springer: New York, 2004; pp 355−371.
(16) Paulsen, H.; Duelund, L.; Zimmermann, A.; Averseng, F. d. r.; Gerdan, M.; Winkler, H.; Toftlund, H.; Trautwein, A. X. *Monatsh. Chem.* **2003**, *134*, 295−306.
(17) Reiher, M. *Inorg. Chem.* **2002**, *41*, 6928−6935.
(18) Reiher, M.; Salomon, O.; Artur Hess, B. *Theor. Chem. Acc.* **2001**, *107*, 48−55.
(19) Salomon, O.; Reiher, M.; Hess, B. A. *J. Chem. Phys.* **2002**, *117*, 4729−4737.
(20) Swart, M. *J. Chem. Theory Comput.* **2008**, *4*, 2057−2066.
(21) de Graaf, C.; Sousa, C. *Chem.—Eur. J.* **2010**, *16*, 4550−4556.
(22) Bolvin, H. *J. Phys. Chem. A* **1998**, *102*, 7525−7534.
(23) Becke, A. D. *J. Chem. Phys.* **1993**, *98*, 5648−5652.
(24) Pierloot, K.; Vancoillie, S. *J. Chem. Phys.* **2008**, *128*, 034104.
(25) Hughes, T. F.; Friesner, R. A. *J. Chem. Theory Comput.* **2011**, 19−32.
(26) Zhao, Y. *J. Chem. Phys.* **2006**, *125*, 194101.
(27) Zhao, Y.; Truhlar, D. G. *Acc. Chem. Res.* **2008**, *41*, 157−167.
(28) Dolg, M.; Wedig, U.; Stoll, H.; Preuss, H. *J. Chem. Phys.* **1987**, *86*, 866−872.
(29) Krishnan, R.; Binkley, J. S.; Seeger, R.; Pople, J. A. *J. Chem. Phys.* **1980**, *72*, 650−654.
(30) Clark, T.; Chandrasekhar, J.; Spitznagel, G. W.; Schleyer, P. V. R. *J. Comput. Chem.* **1983**, *4*, 294−301.
(31) Scalmani, G.; Frisch, M. J. *J. Chem. Phys.* **2010**, *132*, 114110.
(32) Frisch, M. J.; Trucks, G. W.; Schlegel, H. B.; Scuseria, G. E.; Robb, M. A.; Cheeseman, J. R.; Scalmani, G.; Barone, V.; Mennucci, B.; Petersson, G. A.; Nakatsuji, H.; Caricato, M.; Li, X.; Hratchian, H. P.; Izmaylov, A. F.; Bloino, J.; Zheng, G.; Sonnenb, D. J. *Gaussian 09*, revision A.02; Gaussian, Inc.: Wallingford, CT, 2009.
(33) Hohenberg, P.; Kohn, W. *Phys. Rev. B* **1964**, *136*, 864−871.
(34) Becke, A. D. *Phys. Rev. A* **1988**, *38*, 3098−3100.
(35) Perdew, J. P.; Chevary, J. A.; Vosko, S. H.; Jackson, K. A.; Pederson, M. R.; Singh, D. J.; Fiolhais, C. *Phys. Rev. B* **1992**, *46*, 6671−6687.
(36) Becke, A. D. *J. Chem. Phys.* **1993**, *98*, 1372−1377.
(37) Perdew, J. P. *Phys. Rev. B* **1986**, *33*, 8822−8824.
(38) Perdew, J. P.; Wang, Y. *Phys. Rev. B: Condens. Matter* **1992**, *45*, 13244−13249.
(39) Perdew, J.; Burke, K.; Ernzerhof, M. *Phys. Rev. Lett.* **1996**, *77*, 3865−3868.
(40) Perdew, J.; Burke, K.; Ernzerhof, M. *Phys. Rev. Lett.* **1997**, *78*, 1396.
(41) Adamo, C.; Barone, V. *J. Chem. Phys.* **1999**, *110*, 6158−6170.
(42) Bauernschmitt, R.; Ahlrichs, R. *J. Chem. Phys.* **1996**, *104*, 9047−9052.
(43) Seeger, R.; Pople, J. A. *J. Chem. Phys.* **1977**, *66*, 3045−3050.
(44) Ma, B. Q.; Sun, H. L.; Gao, S. *Eur. J. Inorg. Chem.* **2005**, 3902−3906.
(45) Nakayama, Y.; Baba, Y.; Yasuda, H.; Kawakita, K.; Ueyama, N. *Macromolecules* **2003**, *36*, 7953−7958.
(46) Nieuwenhuyzen, M.; Bertram, B.; Gallagher, J. F.; Vos, J. G. *Acta Crystallogr., Sect. C* **1998**, *54*, 603−606.
(47) Alousy, A.; Burgess, J.; Elvidge, D. L. *Transition Met. Chem.* **2005**, *30*, 156−162.
(48) Tang, M. S.; Wu, Y. J.; Liu, X. C.; Du, C. X.; Niu, Y. Y. *Acta Crystallogr., Sect. E: Struct. Rep. Online* **2007**, *63*, m2517−m2517.
(49) Seredyuk, M.; Gaspar, A. B.; Kusz, J.; Bednarek, G.; Gütlich, P. *J. Appl. Crystallogr.* **2007**, *40*, 1135−1145.
(50) Konno, M. M.-K., M. *Bull. Chem. Soc. Jpn.* **1991**, *64*, 339−345.
(51) Ali, A. B.; Grenèche, J.-M.; Leblanc, M.; Maisonneuve, V. *Solid State Sci.* **2009**, *11*, 1631−1638.
(52) Bruno, I. J.; Cole, J. C.; Edgington, P. R.; Kessler, M.; Macrae, C. F.; McCabe, P.; Pearson, J.; Taylor, R. *Acta Crystallogr., Sect. B: Struct. Sci.* **2002**, *58*, 389−397.
(53) Podesta, T. J.; Orpen, A. G. *Cryst. Growth Des.* **2005**, *5*, 681−693.
(54) Dick, S. *Z. Kristallogr.—New Cryst. Struct.* **1998**, *213*, 356.
(55) Sim, P. G.; Sinn, E. *Inorg. Chem.* **1978**, *17*, 1288−1290.
(56) DelaVarga, M.; Petz, W.; Neumu, B.; Costa, R. *Inorg. Chem.* **2006**, *45*, 9053−9063.
(57) Guionneau, P.; Marchivie, M.; Garcia, Y.; Howard, J.; Chasseau, D. *Phys. Rev. B* **2005**, *72*, 1−8.

(58) Medlycott, E. a.; Hanan, G. S.; Abedin, T. S. M.; Thompson, L. K. *Polyhedron* **2008**, *27*, 493−501.
(59) Szalda, D. J.; Creutz, C.; Mahajan, D.; Sutin, N. *Inorg. Chem.* **1983**, *22*, 2372−2379.
(60) Oshio, H.; Spiering, H.; Ksenofontov, V.; Renz, F.; Gutlich, P. *Inorg. Chem.* **2001**, *40*, 1143−1150.
(61) Chang, H. R.; McCusker, J. K.; Toftlund, H.; Wilson, S. R.; Trautwein, A. X.; Winkler, H.; Hendrickson, D. N. *J. Am. Chem. Soc.* **1990**, *112*, 6814−6827.
(62) Romero, R.; Morales, A.; Rodríguez, J.; Bertrán, J. *Transition Met. Chem.* **1992**, *17*, 573−574.
(63) Zhu, H. L.; Xia, D. S.; Zeng, Q. F.; Wang, Z. G.; Wang, D. Q. *Acta Crystallogr., Sect. E: Struct. Rep. Online* **2003**, *59*, m1020−m1021.
(64) Wang, X.-Y.; Justice, R.; Sevov, S. C. *Inorg. Chem.* **2007**, *46*, 4626−4631.
(65) Schilt, A. A. *J. Am. Chem. Soc.* **1960**, *82*, 3000−3005.
(66) Gütlich, P.; Garcia, Y.; Goodwin, H. A. *Chem. Soc. Rev.* **2000**, *29*, 419−427.
(67) Chambers, J.; Eaves, B.; Parker, D.; Claxton, R.; Ray, P. S.; Slattery, S. J. *Inorg. Chim. Acta* **2006**, *359*, 2400−2406.
(68) Khalil, M.; Marcus, M. A.; Smeigh, A. L.; McCusker, J. K.; Chong, H. H. W.; Schoenlein, R. W. *J. Phys. Chem. A* **2006**, *110*, 38−44.
(69) Figgis, B. N.; Hitchman, M. A. *Ligand Field Theory and Its Applications*; Wiley-VCH: New York, 2000; p 354.
(70) Levanon, H.; Stein, G.; Luz, Z. *J. Am. Chem. Soc.* **1968**, *90*, 5292−5293.
(71) Sieber, R.; Decurtins, S.; Stoeckli-Evans, H.; Wilson, C.; Yufit, D.; Howard, J. A. K.; Capelli, S. C.; Hauser, A. *Chem.—Eur. J.* **2000**, *6*, 361−368.
(72) Figgis, B. *Aust. J. Chem.* **1983**, *36*, 1537−1561.
(73) Allen, G.; Warren, K. The electronic spectra of the hexafluoro complexes of the first transition series. In *Struct. Bonding*; Springer: Berlin/Heidelberg, 1971; Vol. *9*, pp 49−138.
(74) Brehm, G.; Reiher, M.; Schneider, S. *J. Phys. Chem. A* **2002**, *106*, 12024−12034.
(75) Brehm, G.; Reiher, M.; Le Guennic, B.; Leibold, M.; Schindler, S.; Heinemann, F. W.; Schneider, S. *J. Raman Spectrosc.* **2006**, *37*, 108−122.
(76) Carter, E. A.; Goddard, W. A. *J. Phys. Chem.* **1988**, *92*, 5679−5683.
(77) Yanagisawa, S.; Tsuneda, T.; Hirao, K. *J. Chem. Phys.* **2000**, *112*, 545−553.
(78) Shaik, S.; Hirao, H.; Kumar, D. *Acc. Chem. Res.* **2007**, *40*, 532−542.